Spin-Crossover Iron(II) Coordination Polymer with Zigzag Chain Structure

Galina S. Matouzenko,*,† Gabor Molnar,‡ Nicolas Bréfuel,‡ Monique Perrin,§ Azzedine Bousseksou,§ and Serguei A. Borshch||,⊥

Stéréochimie et Interactions moléculaires (UMR CNRS and ENS-Lyon 5532), École normale supérieure de Lyon, 46, allée d'Italie, 69364 Lyon Cedex 07, France, Laboratoire de chimie de coordination (UPR CNRS 8241), 205, route de Narbonne, 31077 Toulouse Cedex, France, Laboratoire de reconnaissance et organisation moléculaire (UMR 5078), Université Claude Bernard-Lyon 1, 69622 Villeurbanne Cedex, France, and Institut de Recherches sur la Catalyse, UPR CNRS 5401, 2, avenue Albert Einstein, 69626, Villeurbanne Cedex, France, and Laboratoire de Chimie Théorique et des Matériaux Hybrides, École normale supérieure de Lyon, 46, allée d'Italie, 69364 Lyon Cedex 07, France

Received September 23, 2002. Revised Manuscript Received November 11, 2002

We report on the synthesis and characterization of a first iron(II) spin-crossover coordination polymer of formula $[Fe(pyim)_2(bpy)](ClO_4)_2 \cdot 2C_2H_5OH$, where pyim = 2-(2-pyridyl)imidazole and bpy = 4,4′-bipyridine, with zigzag chain structure. The chains are linked by π stacking into a two-dimensional network. Variable-temperature magnetic susceptibility measurements have revealed the occurrence of the HS ↔ LS transition without hysteresis. The spin conversion temperature $T_{1/2}$ (temperature for which the HS fraction is equal to 0.5) is found equal to 205 K. The crystal structure was resolved at 293 K (high-spin form) and at 173 K (low-spin form). Both spin-state structures belong to the monoclinic space group *C*2/*c* (*Z* = 4). The complex assumes one-dimensional zigzag chain structure, in which the iron(II) active sites are linked to each other by a chemical bridge as the rigid rodlike 4,4′-bipyridine molecule. The Fe−Fe separation via the bpy ligand equals 11.523(2) and 11.201(2) Å in the high-spin and low-spin structures, respectively. The polymeric chains extended along the *c* axis are stacked in the *b* direction forming two-dimensional sheets of bound molecules. The sheets are linked together by several intermolecular H-bonds in the *a* direction. The ensemble of structural features of the complex, potentially leading to the cooperativity, provides a basis for strong interactions. However, they are not strong enough in comparison with the HS−LS energy gap and result in a relatively gradual spin transition of the complex. The structural features and magnetic properties of the complex have been discussed and compared with those for earlier reported iron(II) spin-crossover coordination polymers.

Introduction

The design of new molecular compounds exhibiting a spin-crossover behavior remains one of the most relevant questions in the area of magnetic materials chemistry. The phenomenon of crossover between low-spin (LS) and high-spin (HS) electronic states has been extensively studied during a few past decades and the results have been summarized in several reviews.[1] Potential applications of spin-crossover systems in molecular electronics[1e,f,h,2] require an abrupt spin transition with a relatively large thermal hysteresis, centered near to ambient temperature. Such a magnetic behavior is related to cooperative interactions between the active metal ions in the crystal. Different intermolecular interactions (H-bonding, π stacking, van der Waals contacts) holding together the assemblage of the molecules in the crystal were recognized as leading to pronounced cooperative effects. They serve as information transmitters from one molecule to another when the change of the molecular equilibrium geometry, accompanying a spin transition, occurs. However, due to the noncovalent nature of these cooperative interac-

* Corresponding author. E-mail: Galina.Matouzenko@ens-lyon.fr.
† Stéréochimie et Interactions moléculaires, École normale supérieure de Lyon.
‡ Laboratoire de Chimie de Coordination.
§ Université Claude Bernard-Lyon 1.
|| Institut de Recherches sur la Catalyse.
⊥ Laboratoire de Chimie Théorique et Matériaux Hybrides, École normale supérieure de Lyon.

(1) (a) Goodwin, H. A. *Coord. Chem. Rev.* **1976**, *18*, 293. (b) Gütlich, P. *Struct. Bonding (Berlin)* **1981**, *44*, 83. (c) König, E.; Ritter, G.; Kulshreshtha, S. K. *Chem. Rev.* **1985**, *85*, 219. (d) Toftlund, H. *Coord. Chem. Rev.* **1989**, *94*, 67. (e) Gütlich, P.; Hauser, A. *Coord. Chem. Rev.* **1990**, *97*, 1. (f) Zarembowitch, J.; Kahn, O. *New J. Chem.* **1991**, *15*, 181. (g) König, E. *Struct. Bonding (Berlin)* **1991**, *76*, 51. (h) Gütlich, P.; Hauser, A.; Spiering, H. *Angew. Chem., Int. Ed. Engl.* **1994**, *33*, 2024. (i) Kahn, O. *Molecular Magnetism*; VCH: New York, 1993. (j) Real, J. A. *Transition Metals in Supramolecular Chemistry*; Sauvage, J. P., Ed.; John Wiley & Sons Ltd.: London, 1999.
(2) (a) Kahn, O.; Launay, J. P. *Chemtronics* **1988**, *3*, 140. (b) Kahn, O.; Kröber, J.; Jay, C. *Adv. Mater.* **1992**, *4*, 718.

10.1021/cm021307v CCC: $25.00
Published on Web 12/31/2002

tions, their spreading in the crystal lattice is difficult to control.[3] The idea that the cooperativity should be more pronounced in polymeric compounds, in which the metal active sites are covalently linked by chemical bridges, in regard to mononuclear compounds, was first clearly introduced in ref 4. Supramolecular chemistry and crystal engineering[1i,5] via coordination-driven self-assembly recently gave numerous remarkable examples of construction of metal-containing polymers with specific network topologies.[6] A wide diversity of solid-state architectures including one-dimensional molecular chains and ladders motifs, two-dimensional grids and brick wall structures, and three-dimensional infinite frameworks have already been generated with a simple rigid rodlike spacer such as 4,4′-bipyridine.[6j] These coordination polymers are of considerable actual interest because of their promising catalytic,[7] electrical,[8] optical,[9] and magnetic[10] properties. However, only few iron(II) polymeric compounds manifesting spin-crossover behavior have been reported up to now.[11−16]

In this connection, we attempted to synthesize new polymeric spin-crossover systems via self-assembly of organic molecules with functionally distinct types of nitrogen donor atoms and metal ion building blocks. Here we report the synthesis, structure, and magnetic properties of complex $[Fe(pyim)_2(bpy)](ClO_4)_2 \cdot 2C_2H_5OH$, with pyim = 2-(2-pyridyl)imidazole[17] and bpy = 4,4′-bipyridine. This complex represents the first structurally characterized example of iron(II) spin-crossover coordination polymer with infinite zigzag chains linked by π stacking into a two-dimensional network.

Experimental Section

Chemistry. All reagents and solvents used in this study are commercially available and were used without further purification. All syntheses involving Fe(II) species were carried out in deoxygenated solvents under an inert atmosphere of N_2 using glovebox techniques. The 4,4′-bipyridine was obtained from the Aldrich Chemical Co. 2-(2-Pyridyl)imidazole was prepared as described previously.[17] ^{1}H NMR spectra were recorded in $CDCl_3$ on a Bruker AC200 spectrometer operating at 200 MHz. Elemental analyses (C, H, N, Cl, and Fe determination) were performed at the Service Central de Microanalyse du CNRS in Vernaison.

Synthesis of the Iron(II) Complex. A total of 36.3 mg (0.1 mmol) of $Fe(ClO_4)_2 \cdot 6H_2O$ was dissolved in 3 mL of ethanol, and 15.6 mg (0.1 mmol) of bpy in 2 mL of ethanol was added to it. A light yellow solution was formed. The addition of 29.0 mg (0. 2 mmol) of pyim in 3 mL of ethanol turned the color of this solution to red orange. The solution was filtered and allowed to stand overnight at room temperature, to give red dark crystals of $[Fe(pyim)_2(bpy)](ClO_4)_2 \cdot 2C_2H_5OH$, which were collected by filtration, washed with ethanol, and dried in a vacuum. The crystal used in the X-ray structure determination was selected from this sample. Anal. Calcd for $C_{30}H_{34}N_8Cl_2O_{10}$-Fe: C, 45.42; H, 4.32; N, 14.12; Cl, 8.94; Fe, 7.04. Found: C, 45.33; H, 4.06; N, 14.24; Cl, 9.12; Fe, 6.78.

Caution: Perchlorate salts of metal complexes with organic ligands are potentially explosive. Only small quantities of the compound should be prepared and handled with much care!

Physical Measurements. *Magnetic Properties.* Magnetic susceptibility measurements were carried out using a Faraday-type magnetometer equipped with a continuous-flow Oxford Instruments cryostat. Data were corrected for diamagnetic contributions.

Mössbauer Spectroscopy. The variable-temperature ^{57}Fe Mössbauer measurements were carried out on a constant-acceleration spectrometer with a 50-mCi ^{57}Co(Rh) source. A 50-mg sample of powder was enclosed in a 20-mm-diameter cylindrical plastic sample holder, the size of which has been determined to optimize the absorption. Spectra were obtained in the 80−293 K range using a MD306 cryostat (Oxford Instruments). A least-squares computer program was used to fit the Mössbauer parameters and to determine the standard deviations of statistical origin (given in parentheses). The isomer shift values are given with respect to metallic iron at room temperature.

Solution and Refinement of the X-ray Structure. A Nonius Kappa CCD diffractometer was used for data collection. The selected crystal was sealed in a Lindemann capillary. Two collections were made: the first one at room temperature and the second one at 173 K after a slow decrease of the temperature with a cool dry nitrogen gas stream. From 10 frames with 1° steps, the initial set of cell parameters was obtained for each measurement. A total of 6150 reflections were collected at room temperature of which 3860 unique reflections were used for the structure determination. The second collection at 173 K is formed from 3952 measured reflections, 3775 of which independent reflections were used for the hypothesis and refinement. The structures were solved by direct method by using the SHELXS-97 program.[18] Then the structures were refined by the least-squares method using the SHELXL-97[19]

(3) (a) Matouzenko, G. S.; Bousseksou, A.; Lecocq, S.; van Koningsbruggen, P. J.; Perrin, M.; Kahn, O.; Collet, A. *Inorg. Chem*. **1997**, *36*, 5869. (b) Matouzenko, G. S.; Létard, J.-F.; Bousseksou, A.; Lecocq, S.; Capés, L.; Salmon, L.; Perrin, M.; Kahn, O.; Collet, A. *Eur. J. Inorg. Chem*. **2001**, *11*, 2935.

(4) (a) Kahn, O.; Codjovi, E. *Philos. Trans. R. Soc. London A* **1996**, *354*, 359. (b) Kahn, O.; Garcia, Y.; Letard, J. F.; Mathonière, C. *NATO ASI Ser. C* **1998**, *518*, 127.

(5) (a) Lehn, J. M. *Angew. Chem., Int. Ed. Engl*. **1988**, *27*, 89. (b) Lehn, J. M. *Supramolecular Chemistry*: VCH: Weinheim, Germany, 1995.

(6) (a) Desiraju, G. R. *Angew. Chem., Int. Ed. Engl*. **1995**, *34*, 2311. (b) Batten, S. R.; Robson, R. *Angew. Chem., Int. Ed. Engl*. **1998**, *37*, 1460. (c) Fujita, M.; Ogura, K. *Coord. Chem. Rev*. **1996**, *148*, 249. (d) Fujita, M. *Chem. Soc. Rev*. **1998**, *27*, 417. (e) Blake A. J.; Champness, N. R.; Hubberstey, P.; Li, W.-S.; Withersby, M. A.; Schröder, M. *Coord. Chem. Rev*. **1999**, *183*, 117. (f) Hagrman, P. J.; Hagrman, D.; Zubieta, J. *Angew. Chem., Int. Ed. Engl*. **1999**, *38*, 2638. (g) Zaworotko. M. *Chem. Commun*. **2001**, *1*, 1.

(7) (a) Fujita, M.; Kwon, Y. I.; Washiru, S.; Ogura, K. *J. Am. Chem. Soc*. **1994**, *116*, 1151. (b) *Supramolecular Architecture*; Bein, T., Ed.; ACS Symposium Series 499; American Chemical Society: Washington, DC, 1992.

(8) (a) Ermer, O. *Adv. Mater*. **1991**, *3*, 608. (b) Simon, I.; André. J. J.; Skoulios, A. *New. J. Chem*. **1986**, 295. (c) Hoskins, B. F.; Robson, R. *J. Am. Chem. Soc*. **1990**, *112*, 1546. (d) Bowes, C. L.; Ogin, G. A. *Adv. Mater*. **1996**, *8*, 13.

(9) (a) Chen, C.; Suslick, K. S. *Coord. Chem. Rev*. **1993**, *128*, 293 and references therein. (b) Chiang, W.; Ho, D. M.; Engen, D. V.; Thompson, M. E. *Inorg. Chem*. **1993**, *32*, 2886.

(10) (a) Inoue, K.; Hayamizu, T.; Iwamura, H.; Hashizume, D.; Ohashi, Y. *J. Am. Chem. Soc*. **1996**, *118*, 1803. (b) Strumpf, H. O.; Quahab, L. Q.; Pey, Y.; Grandjean, D.; Kahn, O. *Science* **1993**, *261*, 447. (c) Tamaki, H.; Zhong, Z. J.; Matsumoto, N.; Kida. S.; Keikawa, M.; Ashiwa, N.; Hamimoto, Y.; Okawa, H. *J. Am. Chem. Soc*. **1992**, *114*, 6974. (d) Lloret, F.; Munno, G. D.; Julve, M.; Cano, J.; Ruiz, R.; Caneschi, A. *Angew. Chem., Int. Ed. Engl*. **1998**, *37*, 135. (e) Kumagai, H.; Inoue, K. *Angew. Chem., Int. Ed. Engl*. **1999**, *38*, 1601. (f) Brandon, E. J.; Arif, A. M.; Burkhart, B.; Miller, J. S. *Inorg. Chem*. **1998**, *37*, 2792. (g) Retting, S. J.; Storr, A.; Summers, D. A.; Thompson, R.; Trotter, J. S. *J. Am. Chem. Soc*. **1997**, *119*, 8675. (h) Caneschi, A. Gatteschi, D.; Renard, J. P.; Rey, P. Sessoli, R. *Inorg. Chem*. **1989**, *28*, 3314.

(11) Vreugdenhil, W.; van Diemen, J. H.; de Graaff, R. A. G.; Haasnoot, J. G.; Reedjik J.; van der Kraan, A. M.; Kahn, O.; Zarembowitch, J. *Polyhedron* **1990**, *9*, 2971.

(12) Kahn, O.; Martinez, C. J. *Science* **1998**, *279*, 44 and references therein.

(13) Garcia, Y.; Kahn, O.; Rabardel, L.; Chansou, B.; Salmon, L.; Tuchagues, J. P. *Inorg. Chem*. **1999**, *38*, 4663.

(14) van Koningsbruggen, P.; Garsia, Y.; Kahn. O.; Fournès, L.; Kooijman, H.; Spek. A. L.; Haasnoot, J. G.; Moscovici, J.; Provost, K.; Michalowitch, A.; Renz, F.; Gütlich, P. *Inorg. Chem*. **2000**, *39*, 1891.

(15) Real J. A.; Andrés, E.; Munoz, M. C.; Julve M.; Granier T.; Bousseksou, A.; Varret, F. *Science* **1995**, *268*, 265.

(16) Moliner, N.; Munoz, C.; Létard, S.; Solans, X.; Menéndez, N.; Goujon, A.; Varret, F.; Real, J. A. *Inorg. Chem*. **2000**, *39*, 5390.

(17) Chiswell, B.; Lions, F.; Morris, B. *Inorg. Chem*. **1964**, *3*, 110.

Table 1. Crystallographic Data for $[Fe(pyim)_2(bpy)](ClO_4)_2 \cdot 2C_2H_5OH$

	$T = 293$ K	$T = 173$ K
chem formula	$C_{30}H_{34}N_8Cl_2O_{10}Fe$	
fw	793.40	
a, Å	23.625(5)	23.188(5)
b, Å	11.892(2)	11.559(2)
c, Å	16.510(3)	16.256(3)
β, deg	130.09(3)	130.35(3)
V, Å^3	3548(2)	3321(2)
Z	4	4
space group	$C2/c$	$C2/c$
λ, Å	0.710 73	0.710 73
ρ_{calc}, g·cm^{-3}	1.485	1.587
μ, cm^{-1}	6.42	6.86
$R^a[I > 2\sigma(I)]$	0.061	0.060
$wR_2{}^b[I > 2\sigma(I)]$	0.164	0.156

[a] $R = \sum(|F_o| - |F_c|)/\sum|F_o|$. [b] $wR^2 = \{\sum[w(F_o^2 - F_c^2)^2]/\sum[w(F_o^2)^2]\}^{1/2}$.

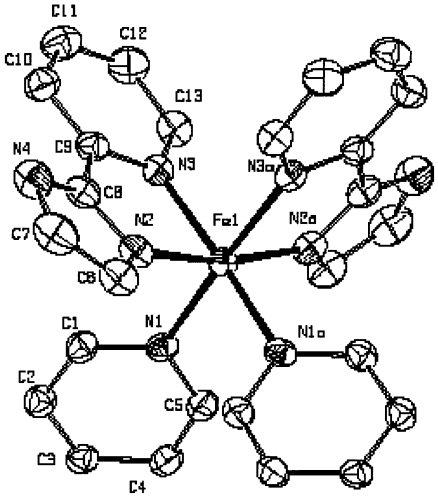

Figure 1. ORTEP drawing of the local coordination of Fe in the cationic unit structure of $[Fe(pyim)_2(bpy)](ClO_4)_2 \cdot 2C_2H_5OH$ at 293 K (ellipsoids enclose 50% probability). The hydrogen atoms are omitted for clarity.

with anisotropic temperature factors for all non-H atoms. The hydrogen atoms were introduced at calculated positions and refined riding on their carrier atoms. The final R factor (with $I > 2\sigma(I)$) has a value of 0.061 and 0.060 for 293 and 173 K, respectively. Crystal data and refinement results are summarized in Table 1. The perspective view of the local coordination of Fe in the cationic unit structure of $[Fe(pyim)_2(bpy)](ClO_4)_2 \cdot 2C_2H_5OH$ has been calculated with PLATON[20] and is shown in Figure 1.

Results

Description of the Structure. The crystal structures of $[Fe(pyim)_2(bpy)](ClO_4)_2 \cdot 2C_2H_5OH$ in both HS and LS states were resolved by X-ray crystallography at 293 K and at 173 K, respectively. The X-ray analysis did not reveal a change in the space group over the temperature range 293−173 K, and both spin-state structures belong to the monoclinic space group $C2/c$ ($Z = 4$). In the crystal, the iron atom lies on a 2-fold rotation axis and the midpoint of the bpy ligand

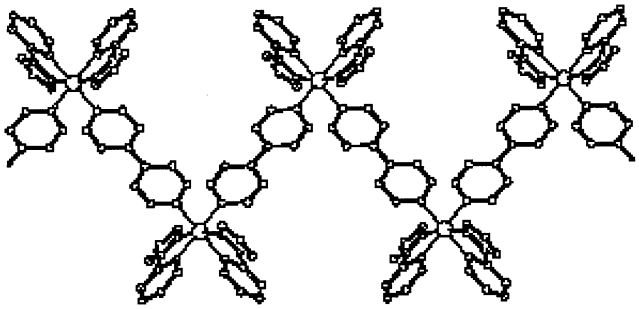

Figure 2. One-dimensional zigzag chain structure of $[Fe(pyim)_2(bpy)](ClO_4)_2 \cdot 2C_2H_5OH$ at 293 K.

Table 2. Selected Bond Distances (Å) and Angles (deg) for $[Fe(pyim)_2(bpy)](ClO_4)_2 \cdot 2C_2H_5OH$[a]

	$T = 293$ K	$T = 173$ K
Fe(1)−N(1)	2.202(3)	2.026 (3)
Fe(1)−N(2)	2.176(3)	2.007(3)
Fe(1)−N(3)	2.217(3)	2.034(3)
N(1)−Fe(1)−N(1)[b]	87.4(2)	88.6(2)
N(1)−Fe(1)−N(2)	95.3(2)	94.3(1)
N(1)−Fe(1)−N(2)[b]	97.4(2)	94.0(1)
N(1)−Fe(1)−N(3)	92.8(1)	92.1(1)
N(1)−Fe(1)−N(3)[b]	173.3(2)	174.7(1)
N(2)−Fe(1)−N(2)[b]	162.5(2)	168.4(2)
N(2)−Fe(1)−N(3)	75.9(2)	80.8(1)
N(2)−Fe(1)−N(3)[b]	91.4(2)	90.8(1)
N(3)−Fe(1)−N(3)[b]	87.9(2)	87.7(2)

[a] Estimated standard deviations in the least significant digits are given in parentheses. [b] Symmetry operation: $-x, y, -z + {}^1/_2$.

coincides with the inversion center. This defines the crystallographically unique unit as a half of the $[Fe(pyim)_2(bpy)](ClO_4)_2 \cdot 2C_2H_5OH$ molecule. As shown in Figure 2, the complex assumes one-dimensional zigzag chain structure, which reflects the preference of the iron for cis-arrangement of two bpy ligands rather than trans-configuration leading to a linear building bloc. The $[FeN_6]$ core is formed by six nitrogen atoms belonging to two bidentate pyim ligands and two different bifunctional bpy spacers. Selected bond lengths and angles are given in Table 2. Despite some differences in the corresponding bond lengths and angles in the geometry of the $[FeN_6]$ octahedrons, their configurations are rather similar at both temperatures.

(a) High-Spin Complex Structure ($T = 293$ K). In the coordination polyhedron, the Fe−N distances are rather close (see Table 2). The N−Fe−N angles fall within 75.9(2)−97.4(2)° for the adjacent nitrogen atoms and 162.5(2)−173.3(2)° for the opposite ones, instead of 90 and 180° that would be observed in an ideal octahedron. This strong distortion of the $[FeN_6]$ core from O_h symmetry is certainly due to the steric constraints caused by the coordination of two bidentate ligands.

At room temperature, the perchlorate ion is severely disordered over two sites (Figure 3a). The disordered groups are represented as two tetrahedra with close positions for Cl atoms and eight different positions for oxygen atoms. The site occupation factors for these two disordered groups are 0.6/0.4 (Cl(1)/Cl(11)). The structure of the ethanol molecule, derived from SHELXS-97 program, is ordered regardless of slightly increased values of thermal anisotropic factors.

Figure 4 shows a projection of the structure on the *ac* plane. The polymer chains run along the *c* axis. At 293 K, the Fe−Fe separation and the Fe−Fe−Fe angle

(18) Sheldrick, G. M. *SHELXS-97, Program for Crystal Structure Determination;* University of Göttingen: Germany, 1997.
(19) Sheldrick, G. M. *SHELXL-97, Program for Crystal Structure Refinement;* University of Göttingen: Germany, 1997.
(20) Spek, A. L. *PLATON, A Multipurpose Crystallographic Tool*; Utrecht University: Utrecht, The Netherlands, 1999.

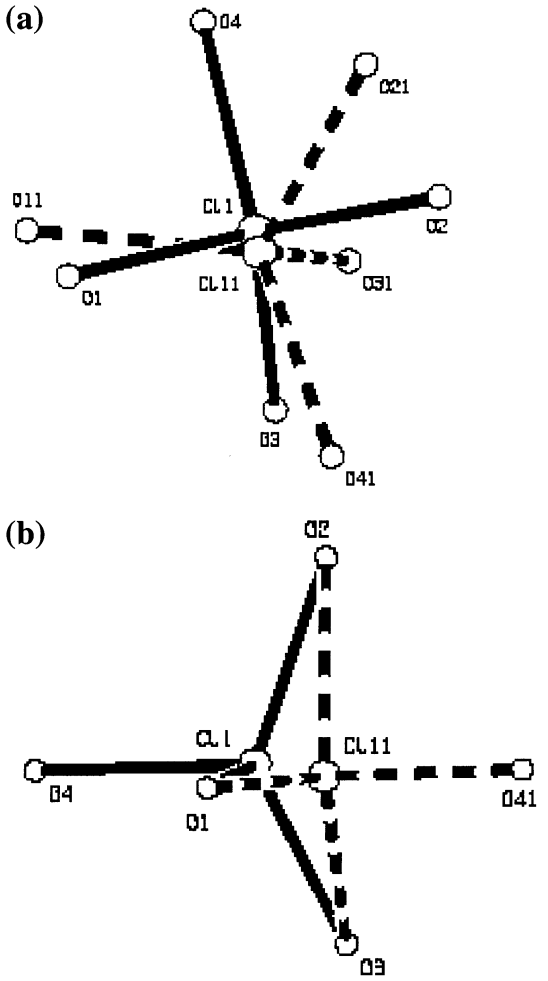

Figure 3. View of the disordered perchlorate ions in [Fe(pyim)$_2$(bpy)](ClO$_4$)$_2$·2C$_2$H$_5$OH at 293 (a) and 173 K (b).

in the chain via the 4,4′-bipyridine ligand are equal to 11.523(2) Å and 91.52(2)°, respectively. The crystal packing of [Fe(pyim)$_2$(bpy)](ClO$_4$)$_2$·2C$_2$H$_5$OH consists of alternate sheets of molecules parallel to the *bc* plane. In a sheet, the X-ray data show a close $\pi-\pi$ stacking between the pyridinic rings of the pyim ligands from the neighboring chains propagating in the *b* direction (symmetry operation: $-x$, $1-y$, $1-z$) (Figure 5). The intermolecular C···C distances (Table 3) connected with the $\pi-\pi$ interactions are rather short and correspond to 3.42−3.48 Å. The interchain Fe−Fe separation in the *bc* plane equals to 9.110(2) Å. The packing of the sheets of molecules creates in their proximity the roughly square channels extended along the *b* direction. The perchlorate anions, located in these channels, link two adjacent cationic sheets of molecules via several H-bonds in the *a* direction (Figure 6). The ethanol molecules interconnect the perchlorate ions arranged in the neighboring channels through the H-bonding. Detailed information on the hydrogen-bonding interactions is listed in Table 4.

(b) Low-Spin Complex Structure (T = 173 K). According to the magnetic data (vide infra), the complex [Fe(pyim)$_2$(bpy)](ClO$_4$)$_2$·2C$_2$H$_5$OH presents a predominantly LS form at this temperature.

The comparison of the HS and LS complex structures shows that the main difference between them consists in the variation of the octahedral geometry in the [FeN$_6$] core. The HS → LS transition is accompanied by a shortening of the Fe−N bond lengths depending on the chemical nature of the nitrogen atoms (Table 2). In the LS complex, the Fe−N(bpy) distances are shorter by 0.176 Å (Fe1−N1). The reduction of the Fe−N(pyim) distances to the imidazolic and aromatic nitrogen atoms is equal to 0.169 (Fe1−N2) and 0.183 Å (Fe1−N3). The N−Fe−N angles, which are significantly distorted in the HS complex, are closer to 90 and 180° in the LS complex. The range of the N−Fe−N angles in the LS [FeN$_6$] core corresponds to 80.8(1)−94.3(1)° and 168.4(2)−174.7(1)°. As expected, the HS → LS transition is accompanied by the ordering of the FeN$_6$ octahedron geometry. At 173 K, the Fe−Fe separation and the Fe−Fe−Fe angle

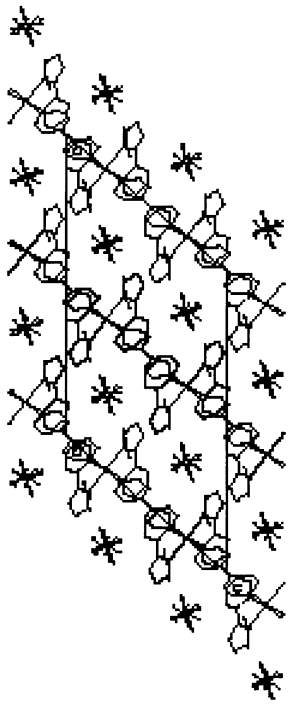

Figure 4. Structure of [Fe(pyim)$_2$(bpy)](ClO$_4$)$_2$·2C$_2$H$_5$OH viewed down the *b* axis at 293 K.

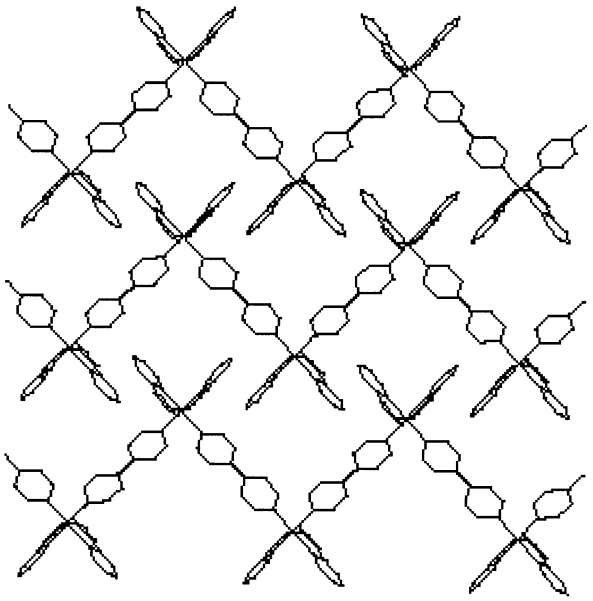

Figure 5. Projection of the molecular structure along the *a* axis for [Fe(pyim)$_2$(bpy)](ClO$_4$)$_2$·2C$_2$H$_5$OH showing the $\pi-\pi$ stacking arrangement at 293 K.

Table 3. Intermolecular C···C Contacts (Å) Shorter than van der Waals Distances (3.6 Å) for $[Fe(pyim)_2(bpy)](ClO_4)_2 \cdot 2C_2H_5OH$[a]

	293 K	123 K
C(11)···C(12)[b]	3.611(7)	3.502(5)
C(12)···C(11)[c]	3.611(7)	3.502(5)
C(11)···C(13)[b]	3.463(6)	3.408(5)
C(13)···C(11)[c]	3.463(6)	3.408(5)
C(12)···C(12)[b]	3.425(10)	3.359(8)
C(12)···C(13)[b]	3.483(7)	3.533(5)
C(13)···C(12)[c]	3.483(7)	3.533(5)

[a] Estimated standard deviations in the least significant digits are given in parentheses. [b] Symmetry operation: $-x, 1-y, 1-z$. [c] Symmetry operation: $-x, 1-y, 1-z$.

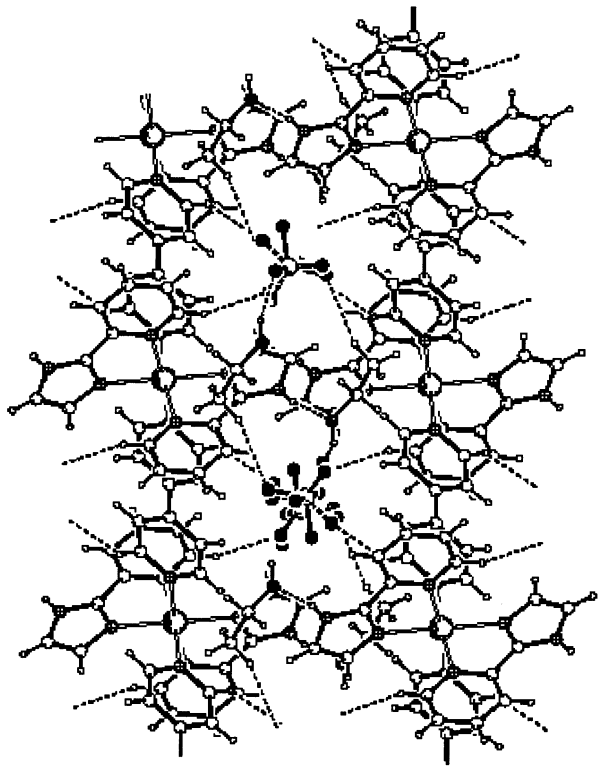

Figure 6. View of $[Fe(pyim)_2(bpy)](ClO_4)_2 \cdot 2C_2H_5OH$ showing the network formed by the hydrogen bonds.

in the polymeric chain are 11.201(2) Å and 93.04(2)°, respectively.

At this temperature, the disorder of perchlorate ions over two sites is retained, but the structure of the disordered elements is changed (Figure 3b). Two disordered tetrahedra with close coordinates for the Cl atoms and common positions for three oxygen atoms display for the forth oxygen atoms two different Cl−O orientations ("up" and "down") along the 3-fold axis. The occupancy ratio for these two disordered groups is 0.8/0.2 (Cl(1)/Cl(11)). It is quite surprising that the ethanol molecule, being only agitated at room temperature, shows a disorder at 173 K. There are two positions for the ethyl group with the site occupation factors as 0.7/0.3 (C(101)/C(102)).

The HS → LS transition is accompanied by a decrease of the unit cell volume by 227 $Å^3$ (6.4%) and an increase in the density from 1.485 to 1.587 g/cm^3. We must note that the volume change is quite important, attesting to a high plasticity of the crystal. A similar value was found earlier for *cis*-bis(thiocyanato)bis[(*N*-2′-pyridylmethylene)-4-(phenylethynyl)aniline]iron(II).[21] On cooling, the anisotropy in the unit cell contraction corresponds to 1.85, 2.80, and 1.54% for the *a*, *b*, and *c* axes, respectively. At 173 K, the crystal packing is similar to that in the HS state. The intermolecular C···C distances (3.35−3.52 Å) and corresponding Fe−Fe separation (8.994(2) Å) between the π stacked neighboring chains become shorter relative to the HS structure. It appears that the $\pi-\pi$ interactions in the sheets of molecules parallel to the *bc* planes are more effective in the LS structure, being in line with the largest variation of the *b* parameter on cooling. In contrast, the efficiency of H-bonding in the LS form seems to be slightly reduced due to the diminishing number of H-bonds. Data on the hydrogen-bonding interactions are listed in Table 4.

Table 4. Interatomic Distances (Å) and Angles (deg) for the Hydrogen-Bonding Interactions for $[Fe(pyim)_2(bpy)](ClO_4)_2 \cdot 2C_2H_5OH$ [a]

D−H···A	D−H	H···A	D···A	D−H···A
293 K				
N(4)−H(4A)···O(100)[b]	0.860	2.00(9)	2.855(5)	171(9)
C(1)−H(1)···O(31)[c]	0.930	2.45(9)	3.238(5)	142(9)
C(13)−H(13)···O(2)[d]	0.930	2.53(9)	3.269(5)	136(9)
C(101)−H(10E)···O(1)[e]	0.960	2.59(9)	3.477(5)	154(9)
O(100)−H(100)···O(4)[f]	0.820	1.95(9)	2.733(5)	159(9)
O(100)−H(100)···O(21)[f]	0.820	2.30(9)	2.865(5)	127(9)
173 K				
N(4)−H(4A)···O(100)[b]	0.880	1.92(9)	2.795(5)	174(9)
C(1)−H(1)···O(3)[c]	0.950	2.50(9)	3.351(5)	149(9)
C(11)−H(11)···O(1)[b]	0.950	2.59(9)	3.339(5)	136(9)
C(13)−H(13)···N(2)[g]	0.950	2.52(9)	3.037(5)	115(9)

[a] Estimated standard deviations in the least significant digits are given in parentheses. Symmetry operations: [b] $x, 1-y, 0.5+z$; [c] $0.5-x, 0.5-y; 1-z$; [d] $-0.5+x, 0.5+y, z$; [e] $0.5-x, 0.5-y, -z$; [f] x, y, z; [g] $-x, y, 0.5-z$.

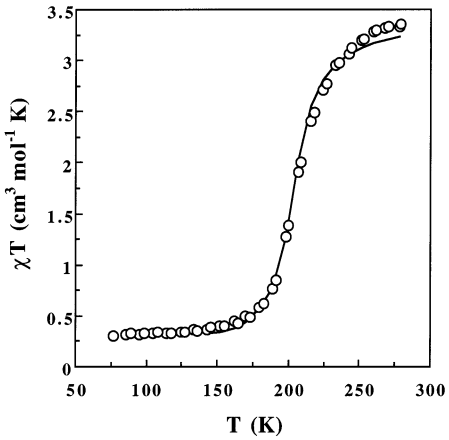

Figure 7. Thermal variation of $\chi_M T$ for $[Fe(pyim)_2(bpy)](ClO_4)_2 \cdot 2C_2H_5OH$. The solid line represents fitted curve.

Magnetic Susceptibility Data. The magnetic properties of the complex are represented in Figure 7 in the form of a $\chi_M T$ versus T plot, where χ_M is the molar magnetic susceptibility and T is the temperature. At 293 K, $\chi_M T$ is equal to 3.4 cm^3 K mol^{-1} and corresponds to a quintet spin state. Just below room temperature, this value decreases gradually upon cooling to 220 K and then descends more steeper to 180 K. The spin conversion temperature $T_{1/2}$ (temperature for which the HS

(21) Guionneau, P.; Létard, J.-F.; Yufit, D.; Chasseau, D.; Bravic, G.; Goeta, A. E.; Howard, J. A. K.; Kahn, O. *J. Mater. Chem.* **1999**, *9*, 985.

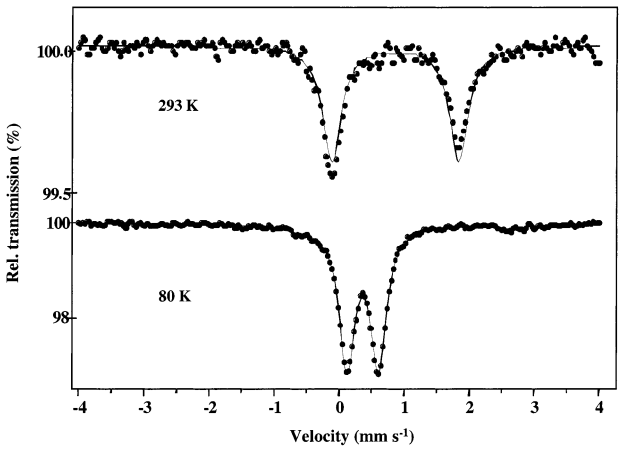

Figure 8. Selected Mössbauer spectra of $[Fe(pyim)_2(bpy)](ClO_4)_2 \cdot 2C_2H_5OH$ recorded in the heating mode. The solid lines represent fitted curves.

fraction is equal to 0.5) is found at 205 K. Upon further cooling of the sample to 77 K, the value of $\chi_M T$ attains 0.31 cm^3 K mol^{-1}. This weak paramagnetism at low temperature may be related to a small residual HS fraction, which can appear due to crystal defects, linked to different lengths of the polymeric chains. On the other hand, the temperature-independent paramagnetism expected for LS iron(II) complexes may also contribute to a residual paramagnetism at low temperature. The same magnetic behavior was observed in the warming mode. No thermal hysteresis was found for this relatively gradual spin transition between HS and LS electronic states.

To estimate the thermodynamic parameters of the spin transition, we used the regular solution model of Slichter and Drickamer.[22] It leads to the following equation for the HS molar fraction γ_{HS}

$$\ln[(1 - \gamma_{HS})/\gamma_{HS}] = [\Delta H + \Gamma(1 - 2\gamma_{HS})]/RT - \Delta S/R$$

where ΔH and ΔS are the enthalpy and entropy variations associated with the spin transition and Γ is the interaction parameter characterizing the cooperativity. The residual HS fraction at low temperature was excluded from the iterative relative error minimization routine. A relative error surface displayed a shallow valley of minima partly extended to a region of unrealistically high parameter values. Figure 7 illustrates the fit with the parameters $\Delta H = 14.3$ kJ mol^{-1}, $\Delta S =$ 69.8 J mol^{-1} K^{-1}, $\Gamma = 2.11$ kJ mol^{-1}, which seems to us most relevant. The agreement factor defined as $\sum_i[(\chi_M T)_{i,exp} - (\chi_M T)_{i,calc}]^2 / \sum_i[(\chi_M T)_{i,exp}]^2$ is 1×10^{-3}.

Mössbauer Spectroscopy. Mössbauer spectra of $[Fe(pyim)_2(bpy)](ClO_4)_2 \cdot 2C_2H_5OH$ recorded at 293 and 80 K in the heating mode are shown in Figure 8. The doublets observed at high and low temperature are typical for iron(II) high-spin and low-spin states, respectively. The isomer shift (IS(HS) = 0.95(1) mm s^{-1} and IS(LS) = 0.481(3) mm s^{-1}) and quadrupole splitting values (Δ_Q(HS) = 1.89(3) mm s^{-1} and Δ_Q(LS) = 0.483(5) mm s^{-1}) at 293 and 80 K are in line with previously observed values for iron(II) spin-crossover compounds. The 293 K spectrum evidences the absence of a residual low-spin fraction (within the detection limit), while the 80 K spectrum indicates the presence of a small residual high-spin fraction (about 2−5%). The Mössbauer data are consistent with the magnetic measurements.

(22) Slichter, C. P.; Drickamer, H. G. *J. Chem. Phys.* **1972**, *56*, 2142.

Discussion

The complex $[Fe(pyim)_2(bpy)](ClO_4)_2 \cdot 2C_2H_5OH$ discussed here represents the first structurally characterized example of iron(II) coordination polymer with infinite zigzag chain undergoing the spin-crossover phenomenon. The iron(II) active sites are linked to each other by a chemical bridge as the rigid rodlike 4,4′-bipyridine molecule, whereby the intersite interactions may be efficiently spread. The coordination polyhedron of iron(II) site is completed to octahedral geometry by coordination of two bidentate 2-(2-pyridyl)imidazole molecules. This ligand was first described in ref 17, and its capacity to form mononuclear spin-crossover complexes of the formula $[Fe(pyim)_3]A_2$ (A = monovalent anion) was demonstrated in several publications.[23] For example, the complex $[Fe(pyim)_3](ClO_4)_2 \cdot H_2O$ shows at 293 K a thermal equilibrium between HS and LS electronic states and the magnetic moment value of 2.50 μ_B.

The magnetic measurements for the complex $[Fe(pyim)_2(bpy)](ClO_4)_2 \cdot 2C_2H_5OH$ reveal a relatively gradual spin transition with $T_{1/2} = 205$ K, and no thermal hysteresis effect was detected. Despite this continuous spin conversion, the fitting procedure with the regular solution model yields a rather high absolute value of the cooperativity parameter $\Gamma = 2.11$ kJ mol^{-1}. However, even with such a high value we are quite far from the threshold at which a thermal hysteresis must appear. According to the Slichter and Drickamer model, it must be equal to $2RT_{1/2} = 3.4$ kJ mol^{-1}.

The X-ray analysis confirms the occurrence of intermolecular interactions in the crystal lattice of the complex. The first structural feature that may contribute to the cooperativity is the direct linkage of the iron(II) spin-crossover centers by the bifunctional 4,4′-bipyridine spacer. The Fe−Fe separation via the bpy ligand is rather large and equals 11.523(2) Å in the HS structure. The other structural property favoring cooperative interactions is the intermolecular π stacking via the overlapping pyridinic rings of the pyim ligands (Table 3). The polymeric chains extended along the *c* axis are stacked in the *b* direction (Figure 5), thus forming two-dimensional sheets of bound molecules (parallel to the *bc* plane). The neighboring fitted in zigzag chains give rise to the Fe−Fe interchain distances (9.110(2) Å at room temperature), which are even less than the intrachain ones. No other interactions between the molecules were found in the *bc* plane. The intermolecular interactions between the polymeric chains in the *a* direction are limited by two indirect H-bonds involving the oxygen atoms of the perchlorate anions (Table 4). It can be concluded that the ensemble of structural features mentioned above and potentially leading to cooperativity provides a basis for strong

(23) (a) Goodgame, D. M.; Machado, A. A. S. *Inorg. Chem.* **1969**, *8*, 2031. (b) Eilbeck, W. J.; Holmes, F. *J. Chem. Soc. A* **1967**, 1777. (c) Dosser, P. R.; Eilceck. W. J.; Underhill, A. E. *J. Chem. Soc. A* **1969**, 810. (d) Reeder, K. A.; Dose, E. V.; Wilson, L. J. *Inorg. Chem.* **1978**, *17*, 1071. (e) McGarvey J. L.; Lawthers, I.; Heremans, K.; Toftlund H. *J. Chem. Soc., Chem. Commun.* **1984**, 1575.

interactions. However, they are not strong enough in comparison with the HS−LS energy gap and result in a relatively gradual spin transition in $[Fe(pyim)_2(bpy)](ClO_4)_2 \cdot 2C_2H_5OH$.

The polymeric approach to design the spin-crossover systems exhibiting a strong cooperativity was introduced quite recently;[4] therefore, the number of such compounds remains still limited. The most extensively studied family includes the iron(II) complexes with 1,2,4-triazole-type ligands.[12] The first polymeric structure was established for the compound $[Fe(btr)_2(NCS)_2] \cdot H_2O$ (btr = 4,4′-bis-1,2,4-triazole) representing a two-dimensional grid.[11] It exhibits an abrupt spin transition with thermal hysteresis width up to 21 K. The structural information for $[Fe(trz)_3]A_2 \cdot nH_2O$ (trz = 4-substituted 1,2,4-triazole; A = a monovalent anion) has been deduced only from EXAFS spectroscopy.[24] The structure of the later compounds consists of linear chains in which the iron(II) atoms are triply bridged by triazole ligands and the shortest Fe−Fe separation equals 3.65 Å. Some of the complexes from this family exhibit abrupt spin transitions with thermal hysteresis width up to ∼40 K.[25] The cooperativity in these systems is assumed to arise from a very short Fe−Fe intersite spacing and a rigid Fe−N−N−Fe linkage favoring the efficient spreading of the intersite interactions. Unfortunately, the structural information on the intermolecular interactions in the crystal lattice is not available. Another Fe(II) compound formed by the 4,4′-bis-1,2,4-triazole ligand $[Fe(btr)_3](ClO_4)_2$, with a three-dimensional crystal structure determined by X-ray analysis, has been reported.[13] The Fe−Fe distance via the bistriazole ligand is 8.67 Å. The presence of two slightly different iron(II) sites generates an abrupt two-step spin transition with a plateau. A key role in the spin conversion regime was attributed to the perturbation created by the noncoordinated perchlorate anions participating in the intermolecular H-bonding. Recently, a new compound $[Fe(btzp)_3](ClO_4)_2$ (btzp = 1,2-bis(tetrazole-1-yl)propane) presenting the first X-ray diffraction-characterized Fe(II) linear polymeric chain has been described.[14] The iron(II) ions in the chain are moved apart by 7.3 Å. However, the complex shows a very gradual and incomplete spin transition. The doubling of the Fe−Fe distance in $[Fe(btzp)_3](ClO_4)_2$ relative to $[Fe(trz)_3]A_2 \cdot nH_2O$, the absence of the H-bonding network in the crystal, and, finally, the flexibility of the spacer ligand were supposed to be responsible for a quasi noncooperative magnetic behavior of the complex.

Two following polymeric spin-crossover complexes have been synthesized using the self-assembly of rigid bifunctional N-donating spacer ligands and iron(II) ions. The compound $[Fe(tvp)_2(NCS)_2] \cdot CH_3OH$ (tvp = 1,2-di(4-pyridyl)ethylene) represents the first catenane supramolecular system showing the occurrence of two perpendicular, fully interlocked two-dimensional networks (Fe−Fe = 13.66 Å).[15] Nevertheless, the spin transition has a gradual and incomplete character, depending also on the sample preparation. The second complex $[Fe(bpb)_2(NCS)_2] \cdot 0.5CH_3OH$ (bpb = 1,4-bis(4-pyridyl)butadiyne) is a singular example of the interpenetration of three mutually perpendicular nets.[16] It displays the occurrence of 50% gradual spin conversion related to the presence of two iron(II) sites in the crystal lattice. The Fe−Fe separations at two sites through the bpb ligand are 16.628 and 16.313 Å.

This restricted number of iron(II) spin-crossover coordination polymers has demonstrated, nevertheless, a relatively wide diversity of architectures such as one-, two-, and three-dimensional structures, as well as a variety of their magnetic behaviors. Some of them, for example, the compound $[Fe(btr)_2(NCS)_2] \cdot H_2O$[11] and a series of complexes $[Fe(trz)_3]A_2 \cdot nH_2O$,[12] directly support the idea that cooperativity in polymer structures, in which the spin-crossover metal sites are linked to each other by chemical bridges, may be enhanced. However, the aforesaid examples also clearly indicate that the simple linking of active sites in the polymeric network is not a solely sufficient condition to generate systems with the cooperative character of spin transition. In particular, it may be supposed that the enhancement of spacing between the active iron(II) sites through the polymeric chain does not affect favorably the intersite interactions. However, the presence of the effective intermolecular interactions such as H-bonding and/or π stacking, as well as the rigidity and conjugated nature of the chemical bridges, favoring the efficient spreading of the intermolecular interactions, can induce an effect quite inverse to a spacing in the chain. Indeed, the intrachain spacing of iron(II) ions in $[Fe(btzp)_3](ClO_4)_2$ (7.3 Å)[14] is less than in $[Fe(btr)_3](ClO_4)_2$ (8.67 Å)[13] and in the described here $[Fe(pyim)_2(bpy)](ClO_4)_2 \cdot 2C_2H_5OH$ (11.523(2) Å), but the strength of cooperative interactions is much weaker, probably due to the absence of the interchain cooperative interactions and the nonconjugated flexible construction of the spacer ligand. One can conclude that the occurrence of the cooperative spin transition regime is a versatile function of structural features of the polymeric compound and further extensive studies of such systems are required.

Acknowledgment. We thank L. Grosvalet for technical assistance in the X-ray analysis.

Supporting Information Available: A full presentation of crystallographic data and experimental parameters, atomic positional parameters, anisotropic displacement parameters, and bond lengths and angles in CIF format. This material is available free of charge via the Internet at http://pubs.acs.org.

CM021307V

(24) (a) Michalowitch, A.; Moscovici, J.; Ducourant, J.; Cracco, D.; Kahn, O. *Chem. Mater.* **1995**, *7*, 1833. (b) Michalowitch, A.; Moscovici, J.; Kahn, O. *J. Phys. IV (Paris)* **1997**, *7*, C2−633.

(25) Kröber, J.; Audière, J. P.; Claude, R.; Codjovi, E.; Kahn, O.; Haasnoot, J. G.; Grolière, F.; Jay, C.; Bousseksou, A.; Linarès, J.; Varret, F.; Gonthier-Vassal, A. *Chem. Mater.* **1994**, *6*, 1404.